TSpace Research Repository utoronto.scholaris.ca

# Reactivity of a Piano-Stool Iron Complex toward Boranes

Liang, Q.; Garcia Mayerstein, H. A.; Song, D

**Version** Post-print/Accepted Manuscript

**Citation (Published Version)** Liang, Q.; Garcia Mayerstein, H. A.; Song, D. Reactivity of a Piano-Stool Iron Complex toward Boranes. *Organometallics* **2023**, *42* (9), 816–824.

**DOI** https://doi.org/10.1021/acs.organomet.3c00037

**Publisher's Statement** This document is the Accepted Manuscript version of a Published Work that appeared in final form in Organometallics, copyright © 2023 American Chemical Society after peer review and technical editing by the publisher. To access the final edited and published work see https://doi.org/10.1021/acs.organomet.3c00037.

**How to cite TSpace items**

**Always cite the published version**, so the author(s) will receive recognition through services that track citation counts, e.g. Scopus. If you need to cite the page number of the **author manuscript from TSpace** because you cannot access the published version, then cite the TSpace version **in addition to** the published version using the permanent URI (handle) found on the record page.

**This article was made openly accessible by U of T Faculty.**
**Please tell us how this access benefits you. Your story matters.**

UNIVERSITY OF TORONTO LIBRARIES

# Reactivity of a Piano-Stool Iron Complex toward Boranes

Qiuming Liang, Hector A. Garcia Mayerstein and Datong Song*

Davenport Chemical Research Laboratories, Department of Chemistry, University of Toronto, 80 St. George Street, Toronto, Ontario, M5S 3H6, Canada

**ABSTRACT:** The binding and activation of boranes by transition metal compounds are relevant to catalytic hydroboration reactions. Herein we report the stoichiometric reactivity of a piano-stool iron complex toward a series of boranes, where the joint action of the metal center and the ligand active site has been observed, as well as the catalytic activity of this iron complex toward the hydroboration of various N-heterocycles.

## INTRODUCTION

The partial reduction of N-heteroarenes provides dearomatized N-heterocycles, which are valuable building blocks in synthetic chemistry and important reductants in biochemical transformations.[1] The difficulties associated with the partial reduction of N-heterocycles are (i) breaking the aromaticity of the inert N-heterocycles and (ii) controlling both the regio- and chemoselectivity. Therefore, the quest for mild and selective partial reduction of N-heterocycle has attracted much attention. In the past two decades, considerable progress has been made toward the selective hydrosilylation or hydroboration of N-heteroarenes.[2] Catalytic systems based on transition metals,[3] lanthanides,[4] actinides,[5] bimetallics,[6] and metal-organic frameworks[7] have been developed for the catalytic reduction of N-heterocycles. The recent development of selective methods based upon earth-abundant transition metal[8] and main group[9] catalysts are particularly noteworthy.

Metal−ligand cooperation, where the metal and ligand cooperatively activate chemical bonds,[10,11] has been demonstrated as a viable working mode for the reduction of N-heteroarenes (Chart 1). Oestreich previously developed a cationic Ru(II)−thiolate catalyst (**I**), which enabled the reversible heterolytic cleavage of H−Si bonds toward the 1,4-selective hydrosilylation of pyridines.[12] The Wang group recently reported the 1,2-selective hydroboration of N-heteroarenes using a dinitrogen-bridged diiron complex (**II**) bearing a P,S-bidentate ligand[13a,b] or a piano-stool Ni(II) complex (**III**) bearing a P,O-bidentate ligand.[13c] The same group later reported the catalytic partial transfer hydrogenation of pyridines and quinolines to N−H 1,4-dihydropyridines[13d] and 1,2-dihydroquinolines,[13e] respectively, using a piano-stool Co(II) complex (**IV**) bearing a P,N-bidentate ligand as the catalyst and $NH_3$•$BH_3$ as the dihydrogen source.

In the abovementioned examples, the metal−ligand cooperactive activation of H−E (E = B or Si) bonds are envisioned as the key step in the catalysis. Our group has long been interested in employing actor ligands in metal complexes toward cooperative bond activations and catalysis.[14] Encouraged by our success on the metal−ligand cooperative activation of $H_2$ and silanes using a piano-stool Fe complex [(Cp*LFe)(μ-$N_2$)(FeCp*L)] (**1**), in which L is a deprotonated N-picolyl-NHC ligand,[14a] we have recently studied the reactvity of **1** toward a series of hydridoboranes. Herein we report the results of these stoichiometric reactions and the subsequent application toward the catalytic hydroboration of N-heteroarenes.

**Chart 1. Dearomative Reduction of N-Heteroarenes via Metal−Ligand Cooperative Catalysis.**

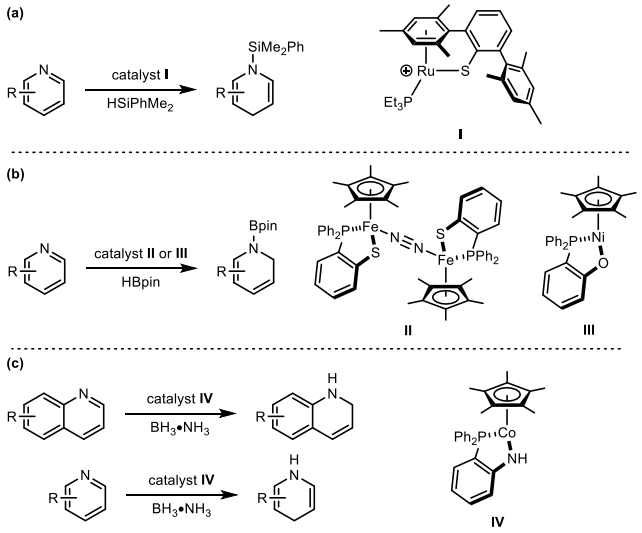


## RESULTS AND DISCUSSION

**Reactivity toward $HBR_2$** Adding two equivalents of $HBR_2$ ($HBCy_2$, 9-BBN, or HBcat) into a THF solution of **1**[14a] at ambient temperature gives the corresponding hydridoborate complexes **2**, **3** and **4**, respectively (Scheme 1) (where Cy is cyclohexyl, 9-BBN is 9-borabicyclo[3.3.1]nonane, and HBcat is catecholborane). The $^1$H NMR spectra show a broad hydride signal at −23.6 ppm for **2**, −21.8 ppm for **3**, and −19.8 ppm for **4**, respectively (Table 1), integrated to one hydride each. The $^{11}$B NMR spectra show one boron signal at 13.8 ppm for **2**, 16.7 ppm for **3**, and 19.7 ppm for **4**, respectively (Table 1). The solid-state structures of **3** and **4** were determined by X-ray crystallography (Figure 1), which revealed the formation of a C−B bond at the nucleophilic pyridylic carbon site of the $L^-$ ligand and a bridging hydride between the boron and iron

center. The pyridine ring regains its aromaticity during this transformation as indicated by the bond lengths around the ring. The Fe−H bond lengths (1.71(2) and 1.60(4) Å for **3** and **4**, respectively) are in the typical range expected for Fe−H[B] distance.[15] The B−H bonds distances are 1.31(2) and 1.28(4) Å for **3** and **4**, respectively. In contrast, when the less hydridic borane $HB(C_6F_5)_2$ was treated with compound **1** at ambient temperature, the resulting product **5** (Figure 1) only had the B−C linkage joining the original **1** and the borane together. The Fe1−H1 distance of 2.58(2) Å is too long even for a 3c-2e bond. In solution, compound **5** features an intermediate-spin Fe(II) center at 25 °C ($\mu_{eff}$ = 3.4 $\mu_B$, $S$ = 1); the $^1$H NMR spectrum of complex **5** in $C_6D_6$ at 25 °C shows paramagnetically broadened and shifted resonances between +46 and −50 ppm. An analogous 16e$^-$ piano-stool iron complex also has an intermediate-spin ($S$ = 1) iron(II) center.[14d]

The addition of two equivalents of pinacolborane (HBpin) to **1** at ambient temperature only converts 0.5 equivalent of **1** into a new diamagnetic product **6**, leaving the other 0.5 equivalent of **1** unreacted. Four equivalents of HBpin can fully convert **1** to **6** at ambient temperature (Scheme 1). The $^1$H NMR spectrum of **6** has two broad hydride signals at −15.9 and −16.5 ppm (Table 1), integrated to one hydride each. The $^{11}$B NMR spectrum has two boron signals at 37.9 and 32.8 ppm (Table 1), diagnostic for two inequivalent boron centers. The solid-state structure of **6** was confirmed by X-ray crystallography (Figure 1), confirming two molecules of HBpin were added to each molecule of **1**. The formation of **6** presumably involves the cooperative B−H bond cleavage across the iron center and the distal pyridylic carbon site of the L$^-$ ligand followed by the addition of HBpin to the resulting iron hydride species, [FeCp*H(L-Bpin)]. The second HBpin is captured by the Fe−H unit to form a $[H_2Bpin]^-$ ligand on Fe in a bidentate mode,[16] displacing the rearomatized pyridine from the metal center. The Fe−B distance of 2.016(3) Å and the Fe−H bond distances of 1.51(3) and 1.54(3) Å are similar to a recently reported analogous complex $[FeCp^*(H_2Bpin)(Ph_2PC_6H_4Bpin)]$.[13f]

**Scheme 1. Reactivity of 1 toward various boranes (Cy = cyclohexyl, Mes = mesityl, HBpin = pinacolborane, HBcat = catecholborane).**

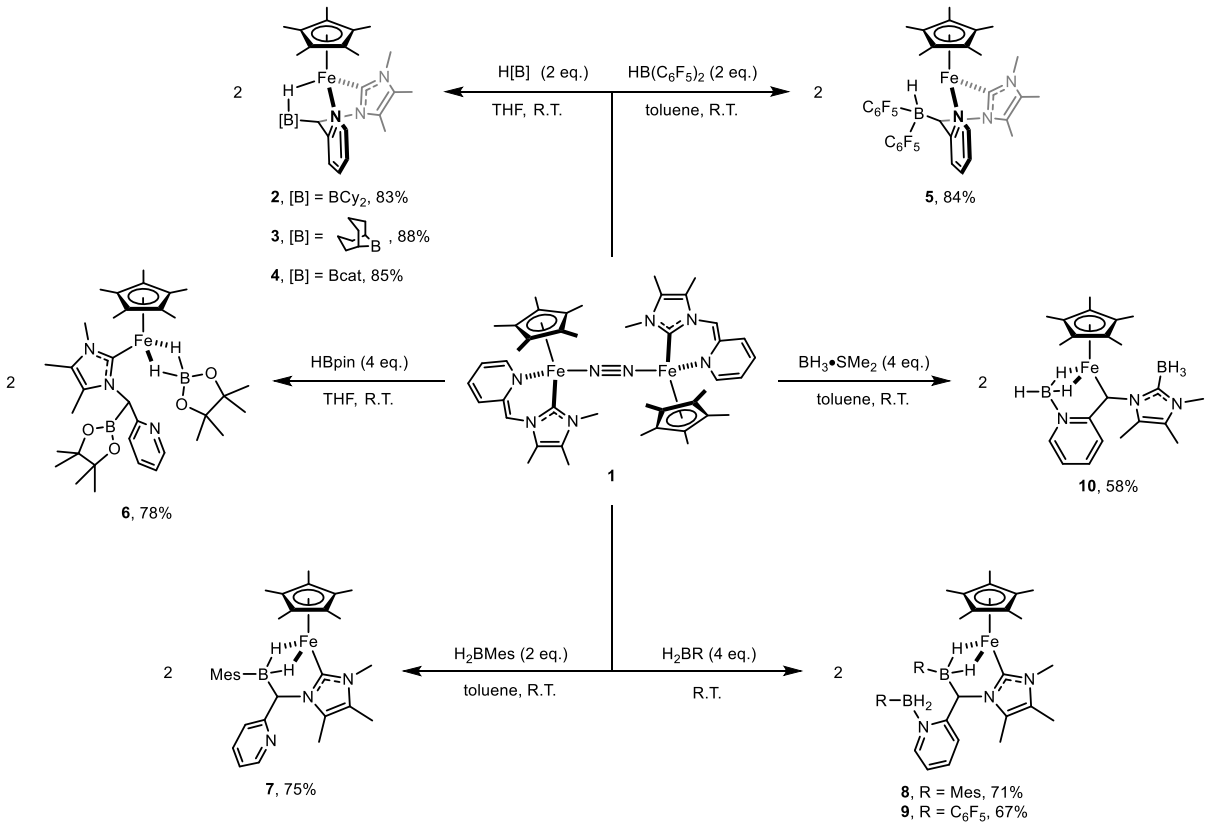


**Table 1. Selected NMR (in $C_6D_6$) data of 2−10.**

| | **2** | **3** | **4** | **5** | **6** | **7** | **8**$^\alpha$ | **9**$^\alpha$ | **10** |
|---|---|---|---|---|---|---|---|---|---|
| $^1$H NMR (B[$\mu$-*H*]$_n$Fe, ppm) | −23.6 | −21.8 | −19.8 | - | −15.9<br>−16.5 | −17.1<br>−17.2 | −17.3<br>−17.5 | −16.6 | −11.7<br>−14.4 |
| $^{11}$B{$^1$H} NMR (ppm) | 13.8 | 16.7 | 19.7 | - | 37.9<br>32.8 | 36.5 | 35.1<br>−12.2 | 23.6<br>−15.6 | 10.9<br>−34.4 |

[a] *In THF-d8.*

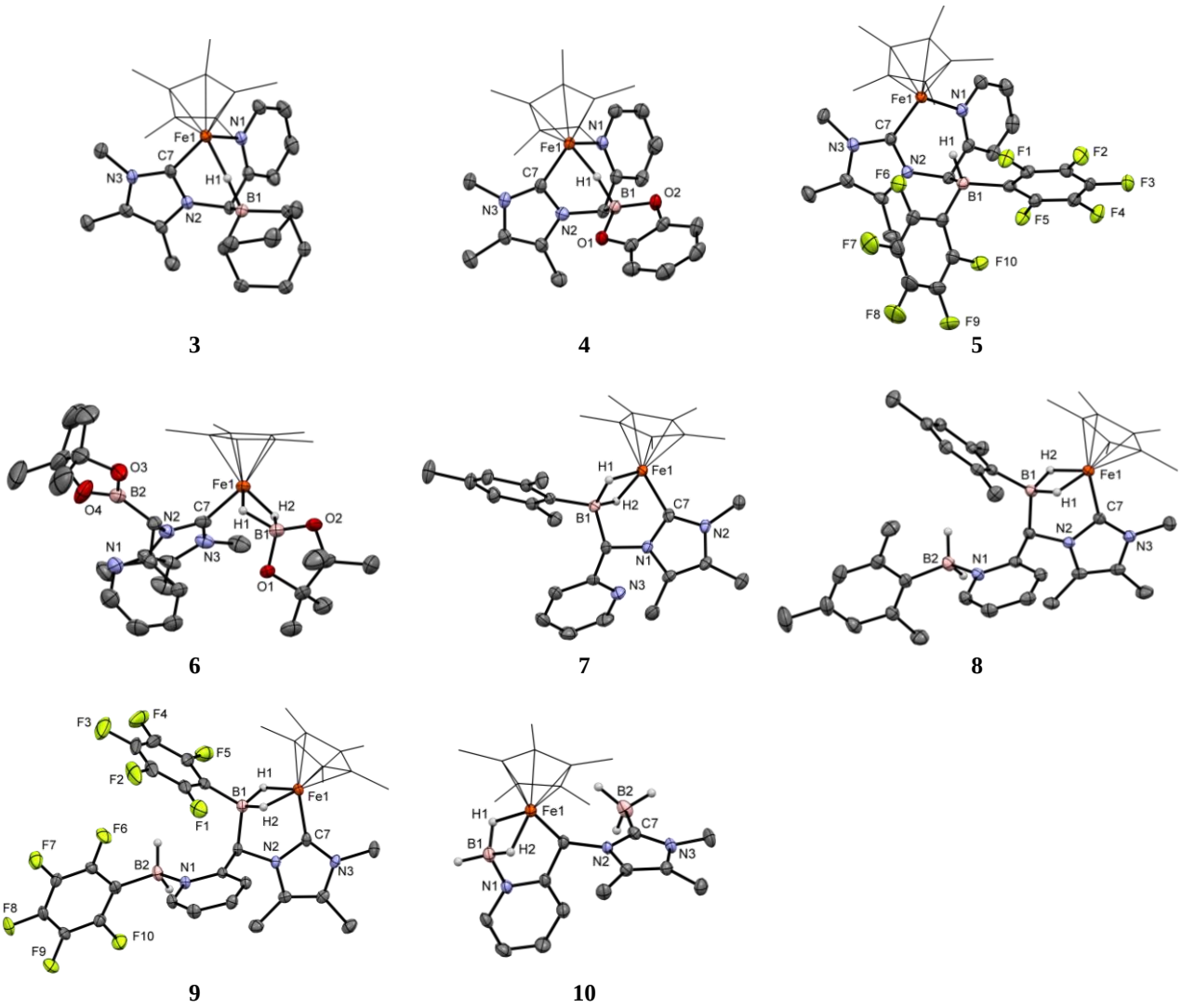


**Figure 1. X-ray structures of 3−10. The thermal ellipsoids are shown at 50% probability. Hydrogen atoms except for the hydrides are omitted and the Cp* ligands are drawn as wireframe for clarity.**

**Reactivity toward $H_2BR$** When complex **1** was treated with two equivalents of $H_2BMes$ (Mes = mesityl) in toluene at ambient temperature, the hydridoborate complex **7** was formed (Scheme 1). The $^1$H NMR spectrum of **7** has two broad hydride signals at −17.1 and −17.2 ppm (Table 1), integrated to one hydride each. The $^{11}$B NMR spectrum shows one boron signal at 36.5 ppm (Table 1). As shown in Figure 1, the X-ray structure of complex **7** indicates that $H_2BMes$ not only forms a B−C bond with the pyridylic carbon of the $L^-$ ligand but also coordinates to the iron center in the bidentate mode with its two hydrides, leaving the rearomatized pyridine moiety of the $L^-$ ligand dangling. In order to form the adduct **8**, where the pyridine N-donor is also bound to a molecule of borane, compound **1** can be reacted with four equivalents of $H_2BMes$ at ambient temperature (Scheme 1). The molecular strucure of **8** was confirmed by X-ray crystallography (Figure 1), showing that the additional $H_2BMes$ was captured by the dangling pyridine of **7**. The pyridine-bound $H_2BMes$ moiety displays a $^{11}$B NMR signal at −12.2 ppm (Table 1), typical for a four-coordinate boron. In contrast, the reaction of **1** and $H_2BC_6F_5$•$SMe_2$ at ambient temperature only produces complex **9**, which has a 2:1 B-to-Fe ratio and resembles **8**. The $^{11}$B NMR spectrum of **9** has two boron signals at 23.6 and −15.6 ppm (Table 1). The adduct that resembles **7** was not observed even if two equivalents of $H_2BC_6F_5$•$SMe_2$ was used to react with **1**, which gives a mixture of **9** and unreacted **1**.

**Reactivity toward $BH_3$•$SMe_2$** Complex **1** reacts with four equivalents of $BH_3$•$SMe_2$ in toluene to yield the hydridoborate complex **10** (Scheme 1), whose molecular structure was established by X-ray crystallography (Figure 1). In this reaction, both the pyridine N-donor and the NHC of the $L^-$ ligand dissociate from the Fe center and each coordinates to a $BH_3$ molecule. The $L^-$ ligand coordinates to the Fe center via its pyridylic carbon. In addition, the N-bound $BH_3$ molecule coordinates to the Fe center in a bidentate fashion via two of its hydrides, whereas the NHC-bound $BH_3$ molecule is terminal. The $^{11}$B NMR spectrum showed two boron signals at 10.9 and −34.4 ppm (Table 1), corresponding to two chemically inequivalent boron centers. By comparing the $^{11}$B NMR spectra of **7** and **8**, we tentatively assign the downfield $^{11}$B NMR signals to the boron centers involved in 3c–2e bonds in compounds **8**–**10**. The two bridging hydrides in **10** (i.e., Fe($\mu$-*H*)$_2$BH) are inequivalent and resonate as two broad doublets at −11.7 and −14.4 ppm (Table 1). The coupling constant between the two bridging hydrides is ~87 Hz. The terminal hydride of the Fe($\mu$-H)$_2$B*H* motif gives rise to a singlet at 2.1 ppm. The NHC-bound $BH_3$ gives rise to a broad signal in the $^1$H NMR at 2.1−2.8 ppm. We were unable to obtain an analytically pure sample of **10** to date. The $^1$H NMR

spectrum of the recrystallized sample of **10** still shows a small amount of impurity, which has not been identified.

**Scheme 2. Hydroboration of *N*-Heteroarenes Catalyzed by Complex 1**[a]

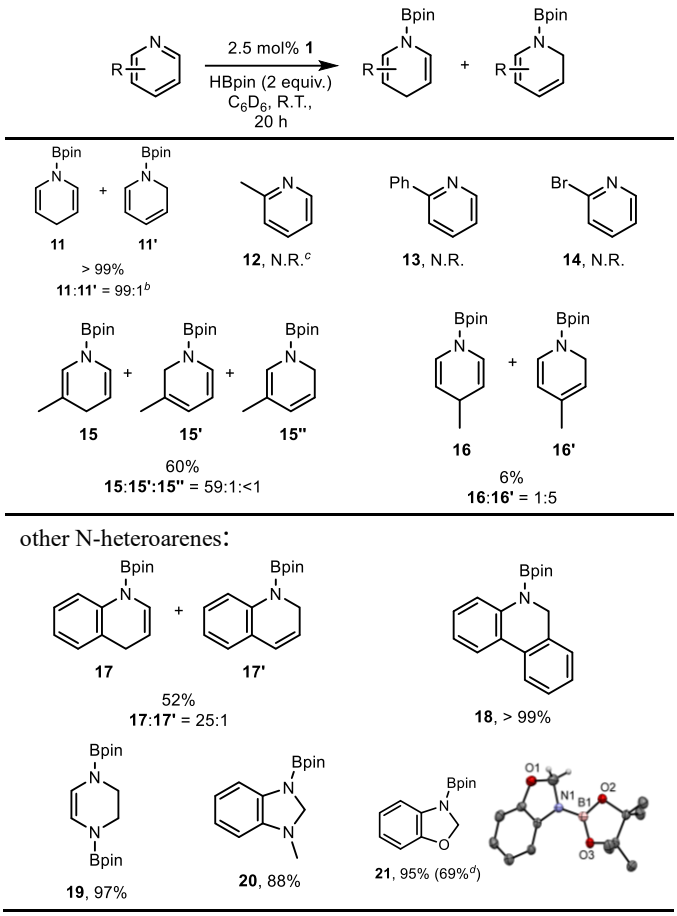


[a] *Reaction conditions: N-heteroarene (0.20 mmol), HBpin (0.40 mmol, 2 equiv.), **1** (2.5 mol %), and tetraethylsilane (internal standard, 0.05 mmol) in 0.6 mL of $C_6D_6$ at room temperature for 20 h. The yields are based on the integration of the products' $^1$H NMR peaks relative to those of the internal standard tetraethylsilane.* [b] *The catalytic reactions using **1** and **6** as the pre-catalysts give comparable results.* [c] *No reaction even at 50 °C.* [d] *Isolated yield for reactions carried out with 1.00 mmol of the substrate and 1.25 mol % of **1**.*

**Catalytic Hydroboration of N-Heterocycles** Given that **1** can cleave the B−H bond in HBpin, we next examined the catalytic activity of **1** toward the hydroboration of pyridines using HBpin. As shown in Scheme 2, with a 2.5 mol % loading of **1** and two equivalents of HBpin in $C_6D_6$ at room temperature under $N_2$, pyridine can be fully converted to the 1,4-hydroborated product (**11**) and 1,2-hydroborated product (**11′**) in a 99:1 ratio within 20 h. The $^{11}$B NMR spectrum of the reaction mixture shows the formation of pinB−O−Bpin byproduct (presumably due to adventitious moisture) along with the hydroboration products. The *ortho*-substituted pyridines (**12**, **13** and **14**) show no reactivity under the same conditions, presumably because of the steric hindrance adjacent to the N-donor. The *meta*-substituted pyridine, 3-methylpyridine, can be coverted to the 1,4-hydroborated product (**15**), 1,2-hydroborated product (**15′**), and 1,6-hydroborated product (**15″**) in a 59:1:<1 ratio. A low conversion (6%) of the *para*-substituted pyridine, 4-methylpyridine was observed, where the 1,4- and 1,2-hydroborated products (**16** and **16′**) were produced in a 1:5 ratio. The reduction of a few other N-heterocycles were explored as well. For example, the hydroboration of quinoline gives a moderate yield of the 1,4-hydroborated product **17** and 1,2-hydroborated product **17′** in a 25:1 ratio. The hydroboration of phenanthridine affords the hydroborated product **18** in a quanitative yield. Interestingly, pyrazine reacts with 2 equivalents of HBpin to afford doubly hydroborylated product **19** in a nearly quantitative yield. Finally, this method was found to be amenable to the reduction of N-methylbenzimidazole and benzoxazole, yielding the corresponding hydroboration products **20** and **21**, respectively, in excellent yields.

Compound **1** reacts with excess pyridine to give a blue complex [Cp*FePyL] (see the Supporting Information), which can be crystallized from the reaction mixture for X-ray crystallographic analysis but loses pyridine under vacuum. However, when both HBpin and pyridine are added in excess, complex **1** is converted to complex **6** exclusively. When compound **6** is mixed with excess pyridine, no reaction was observed in 4 h at room temperature; the partial conversion of **6** to **11** and [Cp*FePyL] was observed after 20 h at room temperature. When compound **6** was mixed with excess HBpin, no reaction was observed in 4 h at room temperature; after 20 h at room temperature, a small amount of a new unidentified iron-containing species was observed in the $^1$H NMR spectrum (see the Supporting Information). During and after the catalytic redution of pyridine, the color of the reaction mixture stays red, similar to the color of compound **6**. The signals of compound **6** are observable in the $^1$H NMR spectrum of the reaction mixture. All these experimental observations suggest that **6** is either an offcycle species or the resting state of the catalytic cycle. Further experiments and computation are needed to elucidate the role of compound **6** in the catalytic reaction mechanism.

## CONCLUSION

In summary, we have explored the reactivity of complex **1** with various hydridoboranes or their $SMe_2$ adducts. With HBcat, $HBCy_2$, and 9-BBN, the reaction occurs at the pyridylic carbon site of the $L^-$ ligand to form a C−B bond, along with formation of a 3c-2e B−H−Fe bond. With reduced hydricity, $HB(C_6F_5)_2$ only forms a C−B bond with the $L^-$ ligand in **1** without formation of a 3c-2e B−H−Fe bond. In contrast, complex **1** cleaves the B−H bond in HBpin across the pyridylic carbon site and the Fe center, resulting in the formation of a C−B bond and an Fe−H bond, which captures another HBpin to form a bidentate borate ligand on the iron center in a facile subsquent step. The C-bound boron center stays three-coordinate. It is interesting to note that the bidentate $[H_2Bpin]^-$ ligand displaces the pyridine N-donor of an N−C chelating ligand from the iron center in this reaction. With $H_2BMes$ and $H_2BC_6F_5$, the formation of a C−B bond brings the two B−H bonds into the coordination sphere of the iron center, displacing the rearomatized Py ring. Compared to the HBpin case, the more Lewis acidic $H_2BMes$ and $H_2BC_6F_5$ can form adducts with the pyridine N-donor, rather than leaving it dangling; the bulkier and less acidic $H_2BMes$ binds with the pyridine N-donor less readily than $H_2BC_6F_5$. The outlier of this series of boranes is $BH_3$, in that, it does not form a C−B bond with the $L^-$ ligand. Instead, $BH_3$ binds with both the pyridine N-donor and the carbene donor, removing both from the iron center. The pyridylic carbon of the $L^-$ ligand coordinates to the iron center. In addition, the N-bound $BH_3$ coordinates to the iron center in the bidentate fashion via two of the three hydrides. Among all the boranes examined in this

work, HBpin is the only one that shows the apparent B−H bond cleavage across the ligand carbon site and the iron center of complex **1**. Moreover we have demonstrated that complex **1** can catalyze the partial hydroboration of various N-heterocycles using HBpin at ambient temperature. Compared to Wang's catalyst, which requires elevated temperature, our catalytic reactions operate at room temperature. Wang's catalyst is compatible with a broader scope of N-heterocycles. Interestingly, the two catalysts show complementary regioselectivity toward the hydroboration of pyridines and quinolines. The mechanism of our catalytic reaction is being investigated in our laboratory.

## EXPERIMENTAL SECTION

Unless stated otherwise all reactions were carried out in a dinitrogen-filled glovebox or using the standard Schlenk techniques under dinitrogen. Glassware was dried in a 180 °C oven overnight. Diethyl ether, hexanes, pentane, and toluene solvents were dried by refluxing and distilling over sodium under dinitrogen. THF solvent was dried by refluxing and distilling over sodium benzophenone ketyl under dinitrogen. $C_6D_6$ and THF-$d_8$ were degassed through three consecutive freeze−pump−thaw cycles. All solvents were stored over 3 Å molecular sieves prior to use. Unless otherwise noted, all NMR spectra were recorded at 25 °C on an Agilent DD2 600 MHz spectrometer or an Agilent DD2 500 MHz spectrometer with a $^{13}$C-sensitive cryogenically cooled probe. Chemical shifts are referenced using the solvent signals. The NMR signal assignments were made based on $^1$H–$^1$H-COSY, $^1$H–$^{13}$C-HSQC, and $^1$H–$^{13}$C-HMBC NMR spectroscopy. Solution magnetic moments were measured at 25 °C by the method originally described by Evans[17] with stock and experimental solutions containing a known amount of a cyclohexane standard. Elemental analyses were carried out at the ANALEST of the University of Toronto. Unless otherwise noted, all chemicals were purchased from commercial sources and used as received. All liquid *N*-heterocycle substrates were distilled over $CaH_2$ and stored over 3A molecular sieves. Compound **1**,[14a] $HBCy_2$,[18] $HB(C_6F_5)_2$,[19] $[H_2BMes]_2$[20] and $H_2BC_6F_5$•$SMe_2$[21] were synthesized according to literatures.

**Complex 2.** To a stirring solution of **1** (202.7 mg, 0.25 mmol) in THF (5 mL) was added a solution of $HBCy_2$ (89.1 mg, 0.50 mmol) in THF (5 mL). The dark brown mixture turned purple immediately. After it was stirred for 3 h, the solution was filtered. The filtrate was concentrated to ∼2 mL, top-layered with 5 mL of *n*-pentane, and cooled to −35 °C to afford a purple crystalline solid of **2**. After the supernatant was decanted off, the solid was washed with *n*-pentane (3 × 1 mL) and dried under vacuum (235.6 mg, 83%). $^1$H NMR (500 MHz, $C_6D_6$) δ 9.54 – 9.46 (m, 1H, py-*H*), 6.69 (td, *J* = 7.4, 1.4 Hz, 1H, py-*H*), 6.64 (dd, *J* = 7.7, 1.6 Hz, 1H, py-*H*), 6.27 (ddd, *J* = 7.4, 6.0, 1.7 Hz, 1H, py-*H*), 3.78 (s, 3H, N-C$H_3$), 3.63 (d, *J* = 4.6 Hz, 1H, C*H*), 2.50 – 2.40 (m, 1H, Cy-*H*), 2.23 (d, *J* = 13.0 Hz, 1H, Cy-*H*), 2.15 – 2.07 (m, 1H, Cy-*H*), 2.03 – 2.00 (m, 1H, Cy-*H*), 1.97 – 1.87 (m, 4H, Cy-*H*), 1.85 (s, 3H, im-C$H_3$), 1.74 (s, 15H, $C_5(CH_3)_5$), 1.72 – 1.65 (m, 2H, Cy-*H*), 1.62 (s, 3H, im-C$H_3$), 1.63 – 1.55 (m, 2H, Cy-*H*), 1.55 – 1.35 (m, 4H, Cy-*H*), 1.31 – 1.12 (m, 4H, Cy-*H*), 0.84 – 0.81 (m, 1H, Cy-*H*), 0.58 – 0.44 (m, 1H, Cy-*H*), 0.32 (t, *J* = 11.2 Hz, 1H, Cy-*H*), −23.59 (s, 1H, Fe(μ-*H*)BCy). $^{13}$C{$^1$H} NMR (126 MHz, $C_6D_6$) δ 194.2 (im-$C^2$), 174.0 (py-*C*), 156.2 (py-*C*), 130.5 (py-*C*), 124.6 (im-*C*), 122.83 (im-*C*), 120.71 (py-*C*), 118.93 (py-*C*), 77.79 ($C_5(CH_3)_5$), 60.8 (*C*H), 36.0 (N-*C*$H_3$), 34.6 (Cy-*C*), 34.0 (Cy-*C*), 33.3 (Cy-*C*), 33.3 (Cy-*C*), 33.2 (br, Cy-*C*), 30.9 (Cy-*C*), 30.7 (Cy-*C*), 30.1 (Cy-*C*), 30.0 (Cy-*C*), 28.9 (Cy-*C*), 28.6 (Cy-*C*), 12.3 ($C_5(CH_3)_5$), 9.8 (im-*C*$H_3$), 9.5 (im-*C*$H_3$). $^{11}$B{$^1$H} NMR (160 MHz, $C_6D_6$) δ 13.8. Anal. Calcd. for $C_{34}H_{52}N_3FeB$: C, 71.71; H, 9.20; N, 7.38. Found: C, 71.78; H, 8.70; N, 6.82.

**Complex 3.** To a stirring solution of **1** (202.7 mg, 0.25 mmol) in THF (5 mL) was added a solution of $(9\text{-BBN})_2$ (61.0 mg, 0.25 mmol) in THF (5 mL). The dark brown mixture turned purple immediately. After it was stirred for 3 h, the solution was filtered. The filtrate was concentrated to ∼2 mL, top-layered with 5 mL of *n*-pentane, and cooled to −35 °C to afford a purple crystalline solid of **3**. After the supernatant was decanted off, the solid was washed with *n*-pentane (3 × 1 mL) and dried under vacuum (226.6 mg, 88%). Crystals suitable for X-ray crystallography were obtained by top-layering a THF solution of **3** with *n*-pentane and cooling to −35 °C. $^1$H NMR (500 MHz, $C_6D_6$) δ 9.61 (dt, *J* = 6.0, 1.1 Hz, 1H, py-*H*), 6.77 (td, *J* = 7.3, 1.4 Hz, 1H, py-*H*), 6.74 – 6.69 (m, 1H, py-*H*), 6.45 (ddd, *J* = 7.1, 5.9, 1.8 Hz, 1H, py-*H*), 3.97 (s, 1H, C*H*), 3.89 (s, 3H, N-C$H_3$), 2.81 – 2.67 (m, 1H, 9-BBN-*H*), 2.53 – 2.26 (m, 3H, 9-BBN-*H*), 2.19 – 2.14 (m, 2H, 9-BBN-*H*), 2.10 – 2.06 (m, 1H, 9-BBN-*H*), 2.02 – 1.85 (m, 5H, 9-BBN-*H*), 1.84 (d, *J* = 0.9 Hz, 3H, im-C$H_3$), 1.82 (s, 15H, $C_5(CH_3)_5$), 1.69 (d, *J* = 0.9 Hz, 3H, im-C$H_3$), 0.56 (s, 1H, 9-BBN-*H*), 0.42 (s, 1H, 9-BBN-*H*), −21.82 (s, 1H, Fe(μ-*H*)BBN). $^{13}$C{$^1$H} NMR (126 MHz, $C_6D$) δ 193.4 (im-$C^2$), 173.1 (py-*C*), 156.7 (py-*C*), 131.1 (py-*C*), 125.0 (im-*C*), 123.8 (im-*C*), 120.0 (py-*C*), 119.2 (py-*C*), 78.8 ($C_5(CH_3)_5$), 61.7 (*C*H), 36.0 (N-*C*$H_3$), 35.2 (9-BBN-*C*), 35.2 (9-BBN-*C*), 34.4 (9-BBN-*C*), 34.2 (9-BBN-*C*), 26.4 (9-BBN-*C*), 26.3 (9-BBN-*C*), 25.6 (9-BBN-*C*), 24.7 (9-BBN-*C*), 12.5 ($C_5(CH_3)_5$), 9.63 (im-*C*$H_3$), 9.61 (im-*C*$H_3$). $^{11}$B{$^1$H} NMR (160 MHz, $C_6D_6$) δ 16.7. Anal. Calcd. for $C_{30}H_{44}N_3FeB$: C, 70.19; H, 8.64; N, 8.19. Found: C, 70.45; H, 8.03; N, 7.59.

**Complex 4.** To a stirring solution of **1** (202.7 mg, 0.25 mmol) in THF (5 mL) was added HBcat (54 μL, 0.50 mmol). The dark brown mixture turned purple immediately. After it was stirred for 3 h, the solution was filtered. The filtrate was concentrated to ∼2 mL, top-layered with 5 mL of *n*-pentane, and cooled to −35 °C to afford a red-purple crystalline solid of **4**. After the supernatant was decanted off, the solid was washed with *n*-pentane (3 × 1 mL) and dried under vacuum (218.3 mg, 85%). Crystals suitable for X-ray crystallography were obtained by top-layering a THF solution of **4** with *n*-pentane and cooling to −35 °C. $^1$H NMR (500 MHz, $C_6D_6$) δ 9.43 (dt, *J* = 5.7, 1.2 Hz, 1H, py-*H*), 7.06 – 6.97 (m, 2H, Bcat-*H*), 6.86 – 6.77 (m, 2H, Bcat-*H*), 6.72 (td, *J* = 7.5, 1.5 Hz, 1H, py-*H*), 6.58 (ddd, *J* = 7.6, 1.6, 0.8 Hz, 1H, py-*H*), 6.32 (ddd, *J* = 7.4, 5.9, 1.6 Hz, 1H, py-*H*), 4.05 (d, *J* = 3.9 Hz, 1H, C*H*), 3.74 (s, 3H, N-C$H_3$), 1.70 (s, 15H, $C_5(CH_3)_5$), 1.62 (d, *J* = 0.9 Hz, 3H, im-C$H_3$), 1.51 (d, *J* = 0.8 Hz, 3H, im-C$H_3$), −19.83 (s, 1H, Fe(μ-*H*)Bcat). $^{13}$C{$^1$H} NMR (126 MHz, $C_6D_6$) δ 192.8 (im-$C^2$), 166.3 (py-*C*), 156.3 (py-*C*), 154.3 (Bcat-*C*), 154.2 (Bcat-*C*), 130.9 (py-*C*), 124.7 (im-*C*), 123.2 (im-*C*), 120.9 (py-*C*), 119.7 (py-*C*), 119.4 (Bcat-*C*), 119.3 (Bcat-*C*), 109.8 (Bcat-*C*), 109.7 (Bcat-*C*), 79.1 ($C_5(CH_3)_5$), 36.0 (N-*C*$H_3$), 12.1 ($C_5(CH_3)_5$), 9.20 (im-*C*$H_3$), 9.17, (im-*C*$H_3$). $^{11}$B{$^1$H} NMR (160 MHz, $C_6D_6$) δ 19.7. Anal. Calcd. for $C_{28}H_{34}N_3FeBO_2$: C, 65.78; H, 6.70; N, 8.22. Found: C, 65.81; H, 6.76; N, 7.98.

**Complex 5.** To a stirring solution of **1** (202.7 mg, 0.25 mmol) in toluene (5 mL) was added a solution of $HB(C_6F_5)_2$ (173.0 mg, 0.50 mmol) in toluene (5 mL). The dark brown mixture turned red immediately. After it was stirred for 3 h, the solution was filtered. The filtrate was concentrated to ∼2 mL, top-layered with 5 mL of *n*-pentane, and cooled to −35 °C to afford an orange solid of **5**, which was collected by filtration, washed with cold ether (3 × 1 mL) and *n*-pentane (3 × 1 mL), and dried under vacuum (315.4 mg, 84%). Crystals suitable for X-ray crystallography were obtained by storing a THF/*n*-pentane solution of **5** at −35 °C. $^1$H NMR (500 MHz, $C_6D_6$) δ 45.87 (1H), 28.85 (1H), 24.71 (15H), 22.81 (3H), 12.03 (3H), −1.04 (1H), −5.05 (1H), −11.01 (3H), −49.56 (1H). $^{19}$F NMR (470 MHz, $C_6D_6$) δ −101.02 (2F), −144.36 (2F), −159.72 (t, *J* = 20.8 Hz, 1F), −159.92 (t, *J* = 20.6 Hz, 1F), −164.73 (t, *J* = 19.4 Hz, 2F), −165.08 (2F). The Evans method (298 K, $C_6D_6$): $\mu_{eff}$ = 3.4 $\mu_B$. Anal. Calcd. for $C_{34}H_{30}N_3FeB_2F_{10}$: C, 55.39; H, 4.10; N, 5.70. Found: C, 55.89; H, 4.26; N, 5.64.

**Complex 6.** To a stirring solution of **1** (202.7 mg, 0.25 mmol) in THF (5 mL) was added HBpin (145 μL, 1.00 mmol). The dark brown mixture turned red immediately. After the mixture was stirred for 3 h and concentrated to dryness under vacuum, the residue was dissolved in 5 mL of *n*-pentane and filtered. The filtrate was concentrated to ∼2 mL, top-layered with 5 mL of hexamethyldisiloxane (HMDSO), and cooled to −35 °C to afford red crystals of **6** that were suitable for X-ray crystallography. After the supernatant was decanted off, the crystals were washed with HMDSO (3 × 1 mL) and dried under vacuum (251.2 mg, 78%). $^1$H NMR (600 MHz, $C_6D_6$) δ 8.39 (ddd, *J* = 4.9, 1.8, 0.8 Hz, 1H, py-*H*), 7.78 (dq, *J* = 8.1, 1.2 Hz, 1H, py-*H*), 7.66 (s, 1H, C*H*), 7.31 – 7.23 (m, 1H, py-*H*), 6.63 (ddt, *J* = 7.4, 4.9, 0.9 Hz, 1H, py-*H*), 3.75 (s, 3H, N-C$H_3$), 2.09 (s, 15H, $C_5(CH_3)_5$), 2.06 (d, *J* = 0.7 Hz (this peak appears as a singlet sometimes), 3H, im-C$H_3$), 1.34 (d, *J*

= 0.7 Hz, 3H, im-C$H_3$), 1.32 (s, 3H, Bpin-C$H_3$), 1.28 (s, 6H, Bpin-C$H_3$), 1.25 (s, 6H, Bpin-C$H_3$), 1.21 (s, 3H, Bpin-C$H_3$), 1.16 (s, 3H, Bpin-C$H_3$), 0.91 (s, 3H, Bpin-C$H_3$), −15.91 (s, 1H, Fe($\mu$-$H$)$_2$Bpin), −16.53 (s, 1H, Fe(μ-$H$)$_2$Bpin). $^{13}$C{$^1$H} NMR (126 MHz, $C_6D_6$) δ 203.5 (im-$C^2$), 162.4 (py-$C$), 147.7 (py-$C$), 136.1 (py-$C$), 126.3 (im-$C$), 126.2 (im-$C$), 124.9 (py-$C$), 121.5 (py-$C$), 84.3 (Bpin-$C$(CH$_3$)$_2$), 82.8 ($C_5$(CH$_3$)$_5$), 80.5 (Bpin-$C$(CH$_3$)$_2$), 79.9 (Bpin-$C$(CH$_3$)$_2$), 55.7 (CH), 36.2 (m, N-CH$_3$), 25.7 – 25.6 (m, Bpin-CH$_3$), 25.3 (Bpin-CH$_3$), 25.2 (m, Bpin-CH$_3$), 25.6 (m, Bpin-CH$_3$), 24.3 (Bpin-CH$_3$), 12.4 – 11.9 (m, ($C_5$(CH$_3$)$_5$)), 11.4 (m, im-CH$_3$), 9.5 – 9.4 (m, im-CH$_3$). $^{11}$B{$^1$H} NMR (192 MHz, $C_6D_6$) δ 37.9, 32.8. Anal. Calcd. for $C_{34}H_{55}N_3FeB_2O_4$: C, 63.09; H, 8.56; N, 6.49. Found: C, 63.34; H, 8.17; N, 6.06.

**Complex 7.** To a stirring solution of **1** (202.7 mg, 0.25 mmol) in toluene (5 mL) was added a solution of $H_2$BMes (66.0 mg, 0.50 mmol) in toluene (5 mL). The dark brown mixture turned light brown gradually. After it was stirred for 3 h, the solution was filtered. The filtrate was concentrated to ~1 mL, top-layered with 5 mL of *n*-pentane, and cooled to −35 °C to afford a pale greenish brown crystalline solid of **7**. After the supernatant was decanted off, the solid was washed with cold ether (3 × 1 mL) and *n*-pentane (3 × 1 mL) and dried under vacuum (197.3 mg, 75%). Crystals suitable for X-ray crystallography were obtained by storing a toluene solution of **7** at −35 °C. $^1$H NMR (500 MHz, $C_6D_6$) δ 8.10 – 8.04 (m, 1H, py-$H$), 7.11 (s, 1H, Mes-$H$), 6.92 (s, 1H, Mes-$H$), 6.76 (td, $J$ = 7.6, 1.9 Hz, 1H, py-$H$), 6.40 (ddd, $J$ = 7.4, 4.8, 1.2 Hz, 1H, py-$H$), 6.16 (d, $J$ = 7.9 Hz, 1H, py-$H$), 4.17 (s, 3H, N-CH$_3$), 3.46 (s, br, 1H, C$H$), 2.77 (s, 3H, Mes-CH$_3$), 2.36 (s, 3H, Mes-CH$_3$), 1.81 (s, 3H, Mes-CH$_3$), 1.73 (s, 18H, overlapping, $C_5$(CH$_3$)$_5$ and im-CH$_3$), 1.25 (d, $J$ = 1.0 Hz, 3H, im-CH$_3$), −17.08 (s, 1H, Fe($\mu$-$H$)$_2$BMes), −17.23 (s, 1H, Fe(μ-$H$)$_2$BMes). $^{13}$C{$^1$H} NMR (126 MHz, $C_6D_6$) δ 196.0 (im-$C^2$), 161.5 (py-$C$), 148.7 (py-$C$), 144.1 (Mes-$C$), 140.6 (Mes-$C$), 139.1 (Mes-$C$), 134.8 (py-$C$ or Mes-$C$), 134.7 (py-$C$ or Mes-$C$), 128.0 (Mes-$C$), 127.9 (Mes-$C$), 125.7 (im-$C$), 125.2 (im-$C$), 120.4 (br, py-$C$), 119.5 (py-$C$), 77.0 ($C_5$(CH$_3$)$_5$), 66.9 (br, $C$H), 35.9 (N-CH$_3$), 23.5 (Mes-CH$_3$), 22.1 (Mes-CH$_3$), 21.5 (Mes-CH$_3$), 12.0 ($C_5$(CH$_3$)$_5$), 9.8 (im-CH$_3$), 9.4 (im-CH$_3$). $^{11}$B{$^1$H} NMR (160 MHz, $C_6D_6$) δ 36.4. Anal. Calcd. for $C_{31}H_{42}N_3FeB$•0.5$Et_2O$: C, 70.73; H, 8.45; N, 7.50. Found: C, 70.24; H, 8.46; N, 7.99.

**Complex 8.** To a stirring solution of **1** (202.7 mg, 0.25 mmol) in toluene (5 mL) was added a solution of $H_2$BMes (132.0 mg, 1.00 mmol) in toluene (5 mL). The reaction mixture was stirred for 3 h, giving a greenish brown suspension. The mixture was then heated to 60 °C to dissolve the product and filtered. The filtrate was concentrated to ~1 mL, top-layered with 5 mL of *n*-pentane, and cooled to −35 °C to afford a pale greenish brown crystalline solid of **8**. After the supernatant was decanted off, the solid was washed with ether (3 × 1 mL) and *n*-pentane (3 × 1 mL) and dried under vacuum (233.1 mg, 71%). Crystals suitable for X-ray crystallography were obtained by cooling a warm (60 °C) saturated benzene solution of **8** to room temperature. $^1$H NMR (500 MHz, THF-$d_8$) δ 7.63 – 7.55 (m, 1H, py-$H$), 7.48 (ddd, $J$ = 8.8, 7.4, 1.7 Hz, 1H, py-$H$), 6.93 (ddd, $J$ = 7.5, 6.1, 1.5 Hz, 1H, py-$H$), 6.78 (s, 1H, Mes-$H$), 6.57 (s, 2H, Mes-$H$), 6.54 (s, 1H, Mes-$H$), 6.24 (ddd, $J$ = 8.2, 1.6, 0.7 Hz, 1H, py-$H$), 4.78 (s, 1H, C$H$), 4.68 (s, 3H, N-CH$_3$), 3.32 (br, s, 1H, Mes-B$H_2$-py), 2.64 (br, s, 1H, Mes-B$H_2$-py), 2.49 (s, 3H, Mes-CH$_3$), 2.24 (s, 3H, im-CH$_3$), 2.22 (s, 3H, Mes-CH$_3$), 2.12 (s, 3H, Mes-CH$_3$), 1.70 (s, 6H, Mes-CH$_3$), 1.65 (s, 15H, $C_5$(CH$_3$)$_5$), 1.60 (s, 3H, im-CH$_3$), 1.57 (s, 3H, Mes-CH$_3$), −17.26 (s, 1H, Fe($\mu$-$H$)$_2$BMes), −17.53 (s, 1H, Fe($\mu$-$H$)$_2$BMes). $^{13}$C{$^1$H} NMR (126 MHz, THF-$d_8$) δ 197.5 (im-$C^2$), 162.6 (py-$C$), 144.8 (py-$C$), 144.0 (Mes-$C$), 140.8 (Mes-$C$), 138.6 (Mes-$C$), 138.4 (Mes-$C$), 134.9 (Mes-$C$), 134.4 (Mes-$C$), 128.2 (Mes-$C$), 127.8 (Mes-$C$), 127.7 (im-$C$), 125.1 (im-$C$), 123.4 (py-$C$), 121.8 (py-$C$), 77.8 ($C_5$(CH$_3$)$_5$), 36.7 (N-CH$_3$), 23.3 (Mes-CH$_3$), 23.1 (Mes-CH$_3$), 22.2 (Mes-CH$_3$), 21.1 (Mes-CH$_3$), 11.7 ($C_5$(CH$_3$)$_5$), 9.4 (im-CH$_3$), 9.3 (im-CH$_3$). $^{11}$B{$^1$H} NMR (192 MHz, THF-$d_8$) δ 35.1, −12.2. Anal. Calcd. for $C_{40}H_{55}N_3FeB_2$•0.5$C_7H_8$: C, 74.49; H, 8.48; N, 5.99. Found: C, 74.56; H, 8.42; N, 6.09.

**Complex 9.** To a stirring solution of **1** (202.7 mg, 0.25 mmol) in toluene (5 mL) was added a solution of $H_2BC_6F_5$•$SMe_2$ (242.0 mg, 1.00 mmol) in toluene (5 mL). The reaction mixture was stirred for 3 h, giving a greenish brown suspension. The mixture was then heated to 60 °C to dissolve the product and filtered. The filtrate was concentrated to ~1 mL, top-layered with 5 mL of *n*-pentane, and cooled to −35 °C to afford a pale greenish brown crystalline solid of **9**. After the supernatant was decanted off, the solid was washed with ether (3 × 1 mL) and *n*-pentane (3 × 1 mL) and dried under vacuum (253.4 mg, 67%). Crystals suitable for X-ray crystallography were obtained by cooling a warm (60 °C) saturated benzene solution of **9** to room temperature. $^1$H NMR (600 MHz, THF-$d_8$) δ 8.29 (m, 1H, py-$H$), 7.76 – 7.63 (m, 1H, py-$H$), 7.24 (m, 1H, py-$H$), 6.17 (m, 1H, py-$H$), 4.74 (s, 3H, N-CH$_3$), 4.18 (s, 1H, C$H$), 3.04 (s, br, py-$H_2BC_6F_5$), 2.66 (s, br, py-$H_2BC_6F_5$), 2.23 (s, 3H, im-CH$_3$), 1.69 (s, 15H, $C_5$(CH$_3$)$_5$), 1.22 (s, im-CH$_3$) −16.55 (s, 2H, Fe($\mu$-$H$)$_2BC_6F_5$). $^{13}$C{$^1$H} NMR (126 MHz, THF-$d_8$) δ 195.3 (im-$C^2$), 161.6 (py-$C$), 148.7 (py-$C$), 140.9 (py-$C$), 128.5 (im-$C$), 125.0 (im-$C$), 123.2 (py-$C$), 122.7 (py-$C$), 77.6 ($C_5$(CH$_3$)$_5$), 36.9 (N-CH$_3$), 11.7 ($C_5$(CH$_3$)$_5$), 9.2 (im-CH$_3$), 8.8 (im-CH$_3$). $^{19}$F NMR (564 MHz, THF-$d_8$) δ −134.47 (d, $J$ = 24.7 Hz, 2F), −134.90 (d, $J$ = 24.9 Hz, 1F), −139.06 (d, $J$ = 25.7 Hz, 1F), −162.73 (t, $J$ = 20.1 Hz, 1F), −163.55 (t, $J$ = 19.9 Hz, 1F), −168.20 (m, 4F). $^{11}$B{$^1$H} NMR (192 MHz, THF-$d_8$) δ 23.6, −15.6. Anal. Calcd. for $C_{34}H_{33}N_3FeB_2F_{10}$: C, 54.37; H, 4.43; N, 5.59. Found: C, 54.51; H, 4.23; N, 5.37.

**Complex 10.** To a stirring solution of **1** (202.7 mg, 0.25 mmol) in toluene (3 mL) was added $BH_3$•$SMe_2$ (95 μL, 1.00 mmol). The dark brown mixture turned blue-purple immediately. After it was stirred for 5 min, the solution was filtered. The filtrate was cooled to −35 °C to afford dark crystals of **10** that were suitable for X-ray crystallography. After the supernatant was decanted off, the crystals were washed with cold toluene (3 × 1 mL) and *n*-pentane (3 × 1 mL) and dried under vacuum (122.4 mg, 58%). $^1$H NMR (500 MHz, $C_6D_6$) δ 7.47 (d, $J$ = 6.2 Hz, 1H, py-$H$), 6.63 (d, $J$ = 8.5 Hz, 1H, py-$H$), 6.35 – 6.21 (m, 1H, py-$H$), 5.80 – 5.64 (m, 1H, py-$H$), 3.92 (s, 1H, C$H$), 3.57 (s, 3H, N-CH$_3$), 2.75 – 2.17 (m, 3H, NHC-B$H_3$), 2.12 (s, 1H, Fe($\mu$-H)$_2$B$H$), 1.85 (s, 15H, $C_5$(CH$_3$)$_5$), 1.67 (s, 6H, im-CH$_3$), −11.71 (d, $J$ = 87.5 Hz, 1H, Fe($\mu$-$H$)$_2$BH), −14.40 (d, $J$ = 86.8 Hz, 1H, Fe($\mu$-$H$)$_2$BH). $^{13}$C{$^1$H} NMR (126 MHz, $C_6D_6$) δ 179.4 (im-$C^2$), 142.3 (py-$C$), 132.1 (py-$C$), 125.6 (im-$C$), 122.9 (im-$C$), 119.8 (py-$C$), 114.2 (py-$C$), 76.9 ($C_5$(CH$_3$)$_5$), 58.7 (CH), 32.5 (N-CH$_3$), 10.9 ($C_5$(CH$_3$)$_5$), 9.2 (im-CH$_3$), 8.4 (im-CH$_3$). $^{11}$B{$^1$H} NMR (192 MHz, $C_6D_6$) δ 10.9, −34.4. Repeated attempts to purify compound **10** failed to yield an analytically pure sample. The $^1$H NMR spectrum of compound **10** shows signals of small amounts of unidentified impurities (See Figure S25 in the Supporting Information). The best elemental analysis rests obtained are given below. Anal. Calcd. for $C_{22}H_{35}N_3FeB_2$: C, 63.06; H, 8.42; N, 10.03. Found: C, 61.55; H, 8.20; N, 10.02.

**General procedures for the catalytic hydroboration of N-heteroarenes.** NMR scale: In a dinitrogen-filled glovebox, a $C_6D_6$ solution of **1** ($1.0 \times 10^{-2}$ M, 0.5 mL, 2.5 mol %) was added to a 2-dram borosilicate glass vial charged with N-heteroarene (0.20 mmol, 1 equiv.), HBpin (58 $\mu$L, 0.40 mmol, 2 equiv.) and tetraethylsilane (9.5 $\mu$L, 0.05 mmol). The reaction was stirred at room temperature for 20 h. The solution was filtered and analyzed by $^1$H NMR spectroscopy to determine the yield of the hydroborated product.

Preparative scale reaction for **21**: Compound **1** (20.3 mg, 0.0125 mmol, 1.25 mol %), benzoxazole (119.1 mg, 1.00 mmol, 1 equiv.) and HBpin (290 $\mu$L, 2.00 mmol, 2 equiv.) were dissolved in 2.5 mL of toluene in a borosilicate glass vial in a dinitrogen-filled glovebox. After the reaction mixture was stirred for 20 h and concentrated to dryness under vacuum, the residue was dissolved in 10 mL of *n*-pentane and filtered through Celite. The filtrate was concentrated to ~5 mL and cooled to −35 °C to afford colorless crystals of **21** that were suitable for X-ray crystallography. After the supernatant was decanted off, the crystals were washed with cold *n*-pentane (3 × 1 mL) and dried under vacuum (170.2 mg, 69 %). $^1$H NMR (500 MHz, $C_6D_6$) δ 7.45 (ddd, $J$ = 7.6, 1.3, 0.5 Hz, 1H, Ar-$H$), 6.83 – 6.74 (m, 2H, Ar-$H$), 6.68 (td, $J$ = 7.7, 1.3 Hz, 1H, Ar-$H$), 5.58 (s, 2H, OC$H_2$N), 1.02 (s, 12H, C$H_3$). $^{13}$C{$^1$H} NMR (126 MHz, $C_6D_6$) δ 152.40 (Ar-$C$), 135.63 (Ar-$C$), 121.55 (Ar-$C$), 121.46 (Ar-$C$), 112.24 (Ar-$C$), 108.44 (Ar-$C$), 84.95 (OCH$_2$N), 83.34 ($C$(CH$_3$)$_2$), 24.67 (C($C$H$_3$)$_2$). $^{11}$B{$^1$H} NMR (192 MHz, $C_6D_6$) δ 22.76.

## ASSOCIATED CONTENT

### Supporting Information

The Supporting Information is available free of charge on the ACS Publications website at DOI:
Experimental procedures, selected crystallographic data tables, and NMR spectra

### Accession Codes

CCDC 2235666−2235672, 2236837−2236839, and 2251971 contain the supplementary crystallographic data for this paper. These data can be obtained free of charge via ww.ccdc.cam.ac.uk/data_request/cif, or by emailing data_request@ccdc.cam.ac.uk, or by contacting The Cambridge Crystallographic Data Centre, 12 Union Road, Cambridge CB2 1EZ, UK; fax: +44 1223 336033.

## AUTHOR INFORMATION

### Corresponding Author

* E-mail for D.S.: d.song@utoronto.ca.

### Notes

The authors declare no competing financial interest.

## ACKNOWLEDGMENT

We thank the Natural Sciences and Engineering Research Council (NSERC) of Canada and Kamal Pharmachem Inc. for funding. We also acknowledge the Canadian Foundation for Innovation Project #19119. H. A. G. M. thanks the Mexican National Council for Science and Technology (CONACyt) for a graduate fellowship.

## REFERENCES

(1) (a) Stout, D. M.; Meyers, A. I. Recent advances in the chemistry of dihydropyridines. *Chem. Rev.* **1982**, *82*, 223−243; (b) McSkimming, A.; Colbran, S. B. The coordination chemistry of organo-hydride donors: new prospects for efficient multi-electron reduction. *Chem. Soc. Rev.* **2013**, *42*, 5439−5488; (c) Zheng, C.; You, S. L. Transfer hydrogenation with Hantzsch esters and related organic hydride donors. *Chem. Soc. Rev.* **2012**, *41*, 2498−2518; (d) Johnson, W. S.; Buell, B. G. 1,2-Dihydroquinoline. *J. Am. Chem. Soc.* **1952**, *74*, 4517−4520; (e) Dillard, R. D.; Pavey, D. E.; Benslay, D. N. Synthesis and antiinflammatory activity of some 2,2-dimethyl-1,2-dihydroquinolines. *J. Med. Chem.* **1973**, *16*, 251−253; (f) Mizoguchi, H.; Oikawa, H.; Oguri, H. Biogenetically inspired synthesis and skeletal diversification of indole alkaloids. *Nat. Chem.* **2014**, *6*, 57−64; (g) Engler, T. A.; LaTessa, K. O.; Iyengar, R.; Chai, W.; Agrios, K. Stereoselective syntheses of substituted pterocarpans with anti-HIV activity, and 5-aza-/5-thia-pterocarpan and 2-aryl-2,3-dihydrobenzofuran analogues. *Bioorg. Med. Chem.* **1996**, *4*, 1755−1769; (h). Roche, S. P.; Porco, J. A. Jr. Dearomatization strategies in the synthesis of complex natural products. *Angew. Chem., Int. Ed.* **2011**, *50*, 4068−4093.

(2) (a) Park, S. Recent Advances in Catalytic Dearomative Hydroboration of N-Heteroarenes. *ChemCatChem.* **2020**, *12*, 3170−3185; (b) Chatterjee, B.; Gunanathan, C. Catalytic Dearomative Hydroboration of Heteroaromatic Compounds. *J. Chem. Sci.* **2019**, *131*, 118; (c) Bull, J. A.; Mousseau, J. J.; Pelletier, G.; Charette, A. B. Synthesis of Pyridine and Dihydropyridine Derivatives by Regio and Stereoselective Addition to N-Activated Pyridines. *Chem. Rev.* **2012**, *112*, 2642−2713.

(3) (a) Kaithal, A.; Chatterjee, B.; Gunanathan, C. Ruthenium Catalyzed Regioselective 1,4-Hydroboration of Pyridines. *Org. Lett.* **2016**, *18*, 3402−3405; (b) Oshima, K.; Ohmura, T.; Suginome, M. Regioselective Synthesis of 1,2-Dihydropyridines by Rhodium-Catalyzed Hydroboration of Pyridines. *J. Am. Chem. Soc.* **2012**, *134*, 3699−3702; (c) Lortie, J. L.; Dudding, T.; Gabidullin, B. M.; Nikonov, G. I. Zinc-Catalyzed Hydrosilylation and Hydroboration of N-Heterocycles. *ACS Catal.* **2017**, *7*, 8454−8459; (d) Wang, X.; Zhang, Y.; Yuan, D.; Yao, Y. Regioselective Hydroboration and Hydrosilylation of N-Heteroarenes Catalyzed by a Zinc Alkyl Complex. *Org. Lett.* **2020**, *22*, 5695−5700; (e) Donnelly, L. J.; Parsons, S.; Morrison, C. A.; Thomas, S. P.; Love, J. B. Synthesis and structures of anionic rhenium polyhydride complexes of boron−hydride ligands and their application in catalysis. *Chem. Sci.* **2020**, *11*, 9994−9999.

(4) Dudnik, A. S.; Weidner, V. L.; Motta, A.; Delferro, M.; Marks, T. J. Atom-efficient regioselective 1,2-dearomatization of functionalized pyridines by an earth-abundant organolanthanide catalyst. *Nat. Chem.* **2014**, *6*, 1100−1107.

(5) Liu, H.; Khononov, M.; Eisen, M. S. Catalytic 1,2-Regioselective Dearomatization of N-Heteroaromatics via a Hydroboration. *ACS Catal.* **2018**, *8*, 3673−3677.

(6) Yu, H.-C.; Islam, S. M.; Mankad, N. P. Cooperative Heterobimetallic Substrate Activation Enhances Catalytic Activity and Amplifies Regioselectivity in 1,4-Hydroboration of Pyridines. *ACS Catal.* **2020**, *10*, 3670−3675.

(7) Ji, P.; Feng, X.; Veroneau, S. S.; Song, Y.; Lin, W. Trivalent Zirconium and Hafnium Metal−Organic Frameworks for Catalytic 1,4-Dearomative Additions of Pyridines and Quinolines. *J. Am. Chem. Soc.* **2017**, *139*, 15600−15603. (b) Ji, P.; Sawano, T.; Lin, Z.; Urban, A.; Boures, D.; Lin, W. Cerium-Hydride Secondary Building Units in a Porous Metal–Organic Framework for Catalytic Hydroboration and Hydrophosphination. *J. Am. Chem. Soc.* **2016**, *138*, 14860−14863.

(8) (a) Tamang, S. R.; Singh, A.; Unruh, D. K.; Findlater, M. Nickel-Catalyzed Regioselective 1,4-Hydroboration of N-Heteroarenes. *ACS Catal.* **2018**, *8*, 6186−6191; (b) Ghosh, P.; Jacobi von Wangelin, A. Manganese-Catalyzed Hydroborations with Broad Scope. *Angew. Chem., Int. Ed.* **2021**, *60*, 16035−16043.

(9) (a) Arrowsmith, M.; Hill, M. S.; Hadlington, T.; Kociok-Köhn, G.; Weetman, C. Magnesium-Catalyzed Hydroboration of Pyridines. *Organometallics* **2011**, *30*, 5556−5559; (b) Fan, X.; Zheng, J.; Li, Z. H.; Wang, H. Organoborane Catalyzed Regioselective 1,4-Hydroboration of Pyridines. *J. Am. Chem. Soc.* **2015**, *137*, 4916−4919; (c) Keyzer, E. N.; Kang, S. S.; Hanf, S.; Wright, D. S. Regioselective 1,4-Hydroboration of Pyridines Catalyzed By An Acid-Initiated Boronium Cation. *Chem. Commun.* **2017**, *53*, 9434−9437; (d) Rao, B.; Chong, C. C.; Kinjo, R. Metal-Free Regio- And Chemoselective Hydroboration of Pyridines Catalyzed By 1,3,2-Diazaphosphenium Triflate. *J. Am. Chem. Soc.* **2018**, *140*, 652−656; (e) Hynes, T.; Welsh, E. N.; Mcdonald, R.; Ferguson, M. J.; Speed, A. W. H. Pyridine Hydroboration with a Diazaphospholene Precatalyst. *Organometallics* **2018**, *37*, 841−844; (f) Jeong, E.; Heo, J.; Park, S.; Chang, S. Alkoxide-Promoted Selective Hydroboration of N-Heteroarenes: Pivotal Roles of *in situ* Generated $BH_3$ in the Dearomatization Process. *Chem. - Eur. J.* **2019**, *25*, 6320−6325; (g) Liu, T.; He, J.; Zhang, Y. Regioselective 1,2-hydroboration of N-heteroarenes using a potassium-based catalyst. *Org. Chem. Front.* **2019**, *6*, 2749−2755; (h) Jeong, J.; Heo, J.; Kim, D.; Chang, S. NHC-Catalyzed 1,2- Selective Hydroboration of Quinolines. *ACS Catal.* **2020**, *10*, 5023−5029; (i) Liu, X.; Li, B.; Hua, X.; Cui, D. 1,2-Hydroboration of Pyridines by Organomagnesium. *Org. Lett.* **2020**, *22*, 4960−4965.

(10) (a) Annibale, V. T.; Song, D. *RSC Adv.* **2013**, *3*, 11432−11449; (b) Khusnutdinova, J. R.; Milstein, D. *Angew. Chem., Int. Ed.* **2015**, *54*, 12236−12273; (c) Elsby, M. R.; Baker, R. T. Strategies and mechanisms of metal-ligand cooperativity in first-row transition metal complex catalysts. *Chem. Soc. Rev.* **2020**, *49*, 8933−8987; (d) Gonçalves, T. P.; Dutta, I.; Huang, K.-W. Aromaticity in catalysis: metal ligand cooperation via ligand dearomatization and rearomatization. *Chem. Commun.* **2021**, *57*, 3070−3082; (e) Gunanathan, C.; Milstein, D. Metal-Ligand Cooperation by Aromatization- Dearomatization: A New Paradigm in Bond Activation and "Green" Catalysis. *Acc. Chem. Res.* 2011, **44**, 588−602.

(11) (a) Rauch, M.; Kar, S.; Kumar, A.; Avram, L.; Shimon, L.; Milstein, D. Metal-Ligand cooperation facilitates bond activation and catalytic hydrogenation with Zinc pincer complexes. *J. Am. Chem. Soc.* **2020**, *142*, 14513−14521; (b) Kumar, A.; von Wolff, N.; Rauch, M.; Zou, Y.-Q.; Shmul, G.; Ben-David, Y.; Leitus, G.; Avram, L.; Milstein, D. Hydrogenative depolymerization of nylons. *J. Am. Chem. Soc.* **2020**, *142*, 14267−14275; (c) Bruffaerts, J.; von Wolff, N.; Diskin-Posner, Y.; Ben-David, Y.; Milstein, D. Formamides as Isocyanate Surrogates. A mechanistically-driven approach to the development of atom efficient, selective catalytic syntheses of ureas, carbamates and heterocycles. *J. Am. Chem. Soc.* **2019**, *141*, 16486−16483;

(d) Das, U. K.; Kumar, A.; Ben-David, Y.; Iron, M. A.; Milstein, D. Manganese catalyzed hydrogenation of carbamates and urea derivatives. *J. Am. Chem. Soc.* **2019**, *141*, 12962−12966.

(12) (a) Omann, L.; Königs, C. D. F.; Klare, H. F. T.; Oestreich, M. Cooperative Catalysis at Metal-Sulfur Bonds. *Acc. Chem. Res.* **2017**, *50*, 1258−1269; (b) Stahl, T.; Müther, K.; Ohki, Y.; Tatsumi, K.; Oestreich, M. Catalytic Generation of Borenium Ions by Cooperative B−H Bond Activation: The Elusive Direct Electrophilic Borylation of Nitrogen Heterocycles with Pinacolborane. *J. Am. Chem. Soc.* **2013**, *135*, 10978−10981; (c) Klare, H. F. T.; Oestreich, M.; Ito, J.-i.; Nishiyama, H.; Ohki, Y.; Tatsumi, K. Cooperative Catalytic Activation of Si−H Bonds by a Polar Ru−S bond: Regioselective Low-Temperature C−H Silylation of Indoles under Neutral Conditions by a Friedel−Crafts Mechanism. *J. Am. Chem. Soc.* **2011**, *133*, 3312−3315; (d) Königs, C. D. F.; Müller, M. F.; Aiguabella, N.; Klare, H. F. T.; Oestreich, M. Catalytic dehydrogenative Si−N coupling of pyrroles, indoles, carbazoles as well as anilines with hydrosilanes without added base. *Chem. Commun.* **2013**, *49*, 1506−1508; (e) Stahl, T.; Klare, H. F. T.; Oestreich, M. C($sp^3$)−F Bond Activation of $CF_3$-Substituted Anilines with Catalytically Generated Silicon Cations: Spectroscopic Evidence for a Hydride-Bridged Ru−S Dimer in the Catalytic Cycle. *J. Am. Chem. Soc.* **2013**, *135*, 1248−1251 (f) Königs, C. D. F.; Klare, H. F. T.; Oestreich, M. Catalytic 1,4-Selective Hydrosilylation of Pyridines and Benzannulated Congeners. *Angew. Chem., Int. Ed.* **2013**, *52*, 10076−10079.

(13) (a) Zhang, F.; Song, H.; Zhuang, X.; Tung, C.-H.; Wang, W. Iron-Catalyzed 1,2-Selective Hydroboration of N-Heteroarenes. *J. Am. Chem. Soc.* **2017**, *139*, 17775−17778; (b) Chen, J.-Y.; Liao, R.-Z. Mechanism and Regioselectivity of the Iron-Catalyzed Hydroboration of N-Heteroarenes: A Computational Study. *Organometallics* **2019**, *38*, 3267−3277; (c) Liu, J.; Chen, J.-Y.; Jia, M.; Ming, B.; Jia, J.; Liao, R.-Z.; Tung, C.-H.; Wang, W. Ni–O Cooperation versus Nickel(II) Hydride in Catalytic Hydroboration of N-Heteroarenes. *ACS Catal.* **2019**, *9*, 3849−3857; (d) Pang, M.; Shi, L.-L.; Xie, Y.; Geng, T.; Liu, L.; Liao, R.-Z.; Tung, C.-H.; Wang, W. Cobalt-Catalyzed Selective Dearomatization of Pyridines to N−H 1,4-Dihydropyridines. *ACS Catal.* **2022**, *12*, 5013−5021; (e) Pang, M.; Chen, J.-Y.; Zhang, S.; Liao, R.-Z.; Tung, C.-H.; Wang, W. Controlled Partial Transfer Hydrogenation of Quinolines by Cobalt-Amido Cooperative Catalysis. *Nat. Commun.* **2020**, *11*, 1249−1257; (f) Sun, R.; Deng, W.-H.; Yu, B.; Lu, Y.; Zhai, X.; Liao, R.-Z.; Tung, C.-H.; Wang, W. Hydroboration of the ($C_5Me_5$)Fe(1,2-$Ph_2PC_6H_4$) System to Derive Hydridoborate and Hydridosilicate Complexes. *Organometallics* **2022**, *41*, 2504−2512.

(14) (a) Liang, Q.; Song, D. Syntheses and Reactivity of Piano-Stool Iron Complexes of Picolyl-Functionalized N-Heterocyclic Carbene Ligands. *Organometallics* **2021**, *40*, 3943−3951; (b) Liang, Q.; Janes, T.; Gjergji, X.; Song, D. Iron complexes of a bidentate picolyl-NHC ligand: synthesis, structure and reactivity. *Dalton Trans.* **2016**, *45*, 13872−13880; (c) Liang, Q.; Osten, K. M.; Song, D. Iron-Catalyzed *gem*-Specific Dimerization of Terminal Alkynes. *Angew. Chem., Int. Ed.* **2017**, *56*, 6317−6320; (d) Liang, Q.; Song, D. Reactivity of Fe and Ru Complexes of Picolyl-Substituted N-Heterocyclic Carbene Ligand: Diverse Coordination Modes and Small Molecule Binding. *Inorg. Chem.* **2017**, *56*, 11956−11970; (e) Liang, Q.; Liu, N. J.; Song, D. Constructing Reactive Fe and Co Complexes from Isolated Picolyl-Functionalized N-Heterocyclic Carbenes. *Dalton Trans.* **2018**, *47*, 9889−9896; (f) Liang, Q.; Salmon, A.; Kim, P. J.; Yan, L.; Song, D. Unusual Rearrangement of an N-Donor-Functionalized N-Heterocyclic Carbene Ligand on Group 8 Metals. *J. Am. Chem. Soc.* **2018**, *140*, 1263−1266.

(15) (a) Hatzis, G. P.; Thomas, C. M. Metal−Ligand cooperativity across two sites of a square planar iron(II) complex ligated by a tetradentate PNNP ligand. *Chem. Commun.* **2020**, *56*, 8611−8614; (b) Deegan, M. M.; Peters, J. C. CO Reduction to $CH_3OSiMe_3$: electrophile-promoted hydride migration at a single Fe site. *J. Am. Chem. Soc.* **2017**, *139*, 2561−2564; (c) Dai, H.; Li, W.; Krause, J. A.; Guan, H. Experimental Evidence of *syn* H−N−Fe−H Configurational Requirement for Iron-Based Bifunctional Hydrogenation Catalysts. *Inorg. Chem.* **2021**, *60*, 6521−6535; (d) Yu, Y.; Brennessel, W. W.; Holland, P. L. Borane B−C Bond Cleavage by a Low-Coordinate Iron Hydride Complex and N–N Bond Cleavage by the Hydridoborate Product. *Organometallics* **2007**, *26*, 3217−3226; (e) Garhwal, S.; Fridman, N.; de Ruiter, G. Z-Selective Alkyne Functionalization Catalyzed by a *trans*-Dihydride N-Heterocyclic Carbene (NHC) Iron Complex. *Inorg. Chem.* **2020**, *59*, 13817−13821; (f) Hatanaka, T.; Ohki, Y.; Tatsumi, K. C−H Bond Activation/Borylation of Furans and Thiophenes Catalyzed by a Half-Sandwich Iron N-Heterocyclic Carbene Complex. *Chem. - Asian J.* **2010**, *5*, 1657−1666; (g) Gorgas, N.; Alves, L. G.; Stöger, B.; Martins, A. M.; Veiros, L. F.; Kirchner, K. Stable, Yet Highly Reactive Nonclassical Iron(II) Polyhydride Pincer Complexes: *Z*-Selective Dimerization and Hydroboration of Terminal Alkynes. *J. Am. Chem. Soc.* **2017**, *139*, 8130−8133.

(16) Janes, T.; Annibale, V. T.; Song, D. Reactivity of Ru(II) and V(III) complexes of diazafluorene derivatives towards B−H bonds. *J. Organomet. Chem.* **2018**, *872*, 79−86.

(17) Evans, D. F. The determination of the paramagnetic susceptibility of substances in solution by nuclear magnetic resonance. *J. Chem. Soc.* **1959**, 2003−2005.

(18) Abiko, A. Dicyclohexylboron Trifluoromethanesulfonate. *Organic Syntheses*, **2003**, *79*, 103−108.

(19) Parks, D. J.; von Spence, R. E.; Piers, W. E. Bis(pentafluorophenyl)borane: Synthesis, Properties, and Hydroboration Chemistry of a Highly Electrophilic Borane Reagent. *Angew. Chem., Int. Ed. Engl.* **1995**, *34*, 809−811.

(20) Smith, K.; Pelter, A.; Jin, Z. Synthesis and Properties of 2,4,6-Trimethylphenylborane (Mesitylborane), a Stable Alternative to Thexylborane. *Angew. Chem., Int. Ed. Engl.* **1994**, *33*, 851−853.

(21) Fuller, A.-M.; Hughes, D. L.; Lancaster, S. J.; White, C. M. Synthesis and Structure of the Dimethyl Sulfide Adducts of Mono- and Bis(pentafluorophenyl)borane. *Organometallics* **2010**, *29*, 2194−2197.